Electronic Supplementary Material (ESI) for Dalton Transactions.

Electronic Supporting Information for

# Heterobimetallic Ba/Li and Ca/Li amides and diphenylmethanide

Erwann le Coz, Hanieh Roueindeji, Vincent Dorcet, Thierry Roisnel,
Jean-François Carpentier and Yann Sarazin*

# Experimental section

## General procedures

All experiments have been performed under inert atmosphere using standard Schlenk techniques or in a dry, solvent-free glove-box (Jacomex; $O_2 < 1$ ppm, $H_2O < 5$ ppm). $CaI_2$ and $BaI_2$ (Aldrich, 99.999%, anhydrous beads) were used as received. $HN(SiMe_2H)_2$ (ABCR) was dried over $CaH_2$ and distilled prior to use. $[Ca\{N(SiMe_2H)_2\}_2]_3$, $[Ba\{N(SiMe_2H)_2\}_2]_n$ and $[LiN(SiMe_2H)_2]_n$ were prepared following the literature protocol.[1] Solvents (pentane and toluene) were purified and dried (water contents all below 10 ppm) over alumina columns (MBraun SPS). The deuterated solvent (Eurisotop, Saclay, France) was stored in sealed ampoules over activated 3 Å molecular sieves and were thoroughly degassed by several freeze–thaw–vacuum cycles. NMR spectra were recorded on a Bruker spectrometer Avance III 400 MHz equipped with a BBOF pulsed field-gradient probe or a Bruker spectrometer Avance 500 MHz equipped with a dual pulse field gradient probehead. All $^1H$ and $^{13}C$ chemicals shifts were determined using residual signals of the deuterated solvents and were calibrated vs. $SiMe_4$. Assignment of the signals was carried out using 1D ($^1H$, $^{13}C\{^1H\}$) and 2D (COSY, edited HSQC and HMBC) NMR experiments. Elemental analyses were performed on a Carlo Erba 1108 Elemental Analyser instrument at the London Metropolitan University by Stephen Boyer and were the average of two independent measurements. However, the extreme air-sensitivity of the complexes precluded the acquisition of reliable and reproducible data sets. Solid-state FTIR spectra were recorded between 400 and 4000 $cm^{-1}$ as Nujol mulls in KBr plates on a Shimadzu IRAffinity-1 spectrometer.

### $[CaLi_2\{\mu^2\text{-}N(SiMe_2H)_2\}_4]_\infty$ (1)

A solution of $[LiN(SiMe_2H)_2]_n$ (0.18 g, 1.3 mmol) in pentane (10 mL) was added dropwise to a solution of $[Ca\{N(SiMe_2H)_2\}_2]$ (0.28 g, 0.65 mmol) in pentane (10 mL). The reaction mixture was stirred at room temperature for 2 h. The solution was then concentrated until precipitation started. The precipitate was then removed by filtration. A crop of colourless X-ray quality crystals (0.23 g, 50%) was obtained from the solution stored overnight at –30 °C.

$^1H$ NMR (benzene-$d_6$, 400.13 MHz, 298 K): $\delta = 4.80$ (overlapping m, 8H, $^1J_{Si–H} \approx 160$ Hz, Si$H$), 0.31 (overlapping s, 48H, SiC$H_3$) ppm.

$^{13}C\{^1H\}$ NMR (benzene-$d_6$, 100.63 MHz, 298 K): $\delta = 4.24$ (Si$C$H$_3$) ppm.

$^7Li$ NMR (benzene-$d_6$, 155.51 MHz, 298 K): $\delta = 1.11$ (minor, 5%), 0.38 (major, 95%) ppm.

$^{29}Si$ NMR (benzene-$d_6$, 79.49 MHz, 298 K): $\delta = –20.78$ ppm.

$^1H$ NMR (thf-$d_8$, 500.13 MHz, 298 K): $\delta = 4.69$-4.67 (overlapping m, 8H, Si$H$), 0.04 (s, 24H, SiC$H_3$), –0.02 (s, 24H, SiC$H_3$) ppm.

$^{13}C\{^1H\}$ NMR (thf-$d_8$, 125.77 MHz, 298 K): δ = 5.84 (Si*C*H$_3$), 5.50 (Si*C*H$_3$) ppm.

FTIR (nujol in KBr plates): $\tilde{\upsilon}_{\text{Si-H}}$ = 2034.90 (s), 1944.25 (s), 1797.66 (m), 1714.72 (w), 1631.78 (m), 1458.18 (s), 1415.75 (w), 1377.17 (s), 1247.94 (s), 1055.06 (s), 1026.13 (w), 962.48 (m), 893.04 (s), 833.28 (m), 752.24 (m), 677.01 (w), 624.94 (w), 584.43 (w) cm$^{-1}$.

**$[Ba_2Li_2\{\mu^2\text{-}N(SiMe_2H)_2\}_6]_\infty$ (2)**

A solution of $[LiN(SiMe_2H)_2]_n$ (34 mg, 0.24 mmol) in toluene (10 mL) was added dropwise to a solution of $[Ba\{N(SiMe_2H)_2\}_2]$ (100 mg, 0.19 mmol) in toluene (10 mL). The reaction mixture was stirred at room temperature for 2 h. The solution was then concentrated until precipitation started. The precipitate was then removed by filtration. A crop of colourless X-ray quality crystals (55 mg, 41%) was obtained from the solution stored overnight at –30 °C.

$^1H$ NMR (benzene-$d_6$, 400.13 MHz, 298 K): δ = 4.92 (s, 12H, $^1J_{\text{Si–H}}$ = 160 Hz, Si*H*), 0.32 (s, 72H, SiC*H*$_3$) ppm.

$^{13}C\{^1H\}$ NMR (benzene-$d_6$, 100.63 MHz, 298 K): δ = 4.16 (Si*C*H$_3$) ppm.

$^7Li$ NMR (benzene-$d_6$, 155.51 MHz, 298 K): *δ* = 0.85 ppm.

$^1H$ NMR (thf-$d_8$, 500.13 MHz, 298 K): δ = 4.68 (m, 12 H, $^1J_{\text{Si–H}}$ = 168 Hz, Si*H*), 0.01 ppm (s, 72 H, SiC*H*$_3$) ppm.

$^{13}C\{^1H\}$ NMR (thf-$d_8$, 125.77 MHz, 298 K): δ = 5.69 (Si*C*H$_3$)ppm.

FTIR (nujol in KBr plates): $\tilde{\upsilon}_{\text{Si-H}}$ = 1994.40 (s), 1930.00 (sh), 1778.37 (m), 1649.14 (w), 1456.26 (s), 1411.88 (w), 1377.17 (s), 1340.53 (w), 1251.80 (s), 1103.28 (m), 1056.99 (m), 972.12 (s), 945.12 (s), 887.26 (m), 831.32 (m), 771.53 (s), 700.16 (w), 678.94 (m), 626.87 (m), 592.15 (m), 561.29 (w) cm$^{-1}$.

**$[LiCHPh_2.tmeda]$**

A solution of *n*BuLi 2.5 M in hexane (10.3 ml, 25.8 mmol) was added dropwise at room temperature to a solution of $Ph_2CH_2$ (4.34 g, 25.8 mmol) and tmeda (3.00 g, 25.8 mmol) in dry pentane (30 mL), resulting in the rapid formation of a non-miscible deep red-orange oil. The mixture was stirred at 30 °C. After 3 h, the mixture spontaneously separated in two phases, the lower one consisting of a deep red-orange oil. The upper phase (pentane) was removed by cannula, and the remaining red-orange oil was then dried under vacuum. The deep red-orange oil crystallised under vacuum to afford a deep orange crystalline solid (6.74 g, 90%). *NB*: the formation of a solid red-orange precipitate may be observed instead of an oil under extremely fast stirring.

$^1H$ NMR (tol-$d_8$, 400.13 MHz, 298 K): *δ* = 7.07-7.03 (m, 4H; *m*-C*H*), 6.95-6.93 (m, 4H; *o*-C*H*), 6.35 (m, 2H; *p*-C*H*), 4.56 (s, 1H; Ph$_2$C*H*), 1.55 (s, 12H; N(C*H*$_3$)$_2$), 1.51 (s, 4H; C*H*$_2$NMe$_2$) ppm.

**$[Li(tmeda)_2^+.Ca(CHPh_2)_3(thf)^-]$ (3)**

A solution of $[LiCHPh_2.tmeda]$ (1.12 g, 3.9 mmol) in $Et_2O$ (6 mL) was added dropwise at room temperature to a solution of $[Ca\{N(SiMe_3)_2\}_2.(thf)_2]$ (0.65 g, 1.3 mmol) in $Et_2O$ (5 mL), resulting in the rapid formation of a non-miscible deep red oil. The mixture was stirred at room temperature. After 12 h, the mixture spontaneously separated in two phases, the lower one consisting of a deep red oil. The upper phase ($Et_2O$) was removed by cannula, and the remaining red oil was further washed with $Et_2O$ (5 mL) and then dried under vacuum. The deep red oil crystallised under vacuum and afforded red single crystals suitable for X-ray analysis (0.74 g, 74%).

$^1$H NMR (thf-$d_8$, 400.13 MHz, 298 K): $\delta$ = 6.73 (m, 24H; *o*- and *m*-C*H*), 6.00 (m, 6H; *p*-C*H*), 3.91 (s, 3H; $Ph_2CH$), 2.35 (s, 8H; $CH_2NMe_2$), 2.19 (s, 24H; $N(CH_3)_2$) ppm.

$^1$H NMR (thf-$d_8$, 400.13 MHz, 213 K): $\delta$ = 6.70 (m, 6H; *m*-C*H*), 6.53 (m, 6H; *m*-C*H*), 6.38 (m, 6H; *o*-C*H*), 6.09 (m, 6H; *o*-C*H*), 5.55 (m, 6H; *p*-C*H*), 4.20 (s, 3H; $Ph_2CH$), 2.26 (s, 8H; $CH_2NMe_2$), 2.12 (s, 24H; $N(CH_3)_2$) ppm.

$^{13}C\{^1H\}$ NMR (thf-$d_8$, 100.63 MHz, 213 K): $\delta$ 146.80, 128.80, 127.44, 121.87, 112.98, 106.29 (all arom-*C*H), 80.22 ($CHPh_2$), 58.91 ($CH_2NMe_2$), 46.43 ($N(CH_3)_2$) ppm.

$^7$Li NMR (thf-$d_8$, 155.51 MHz, 213 K): $\delta$ = –0.57 ppm.

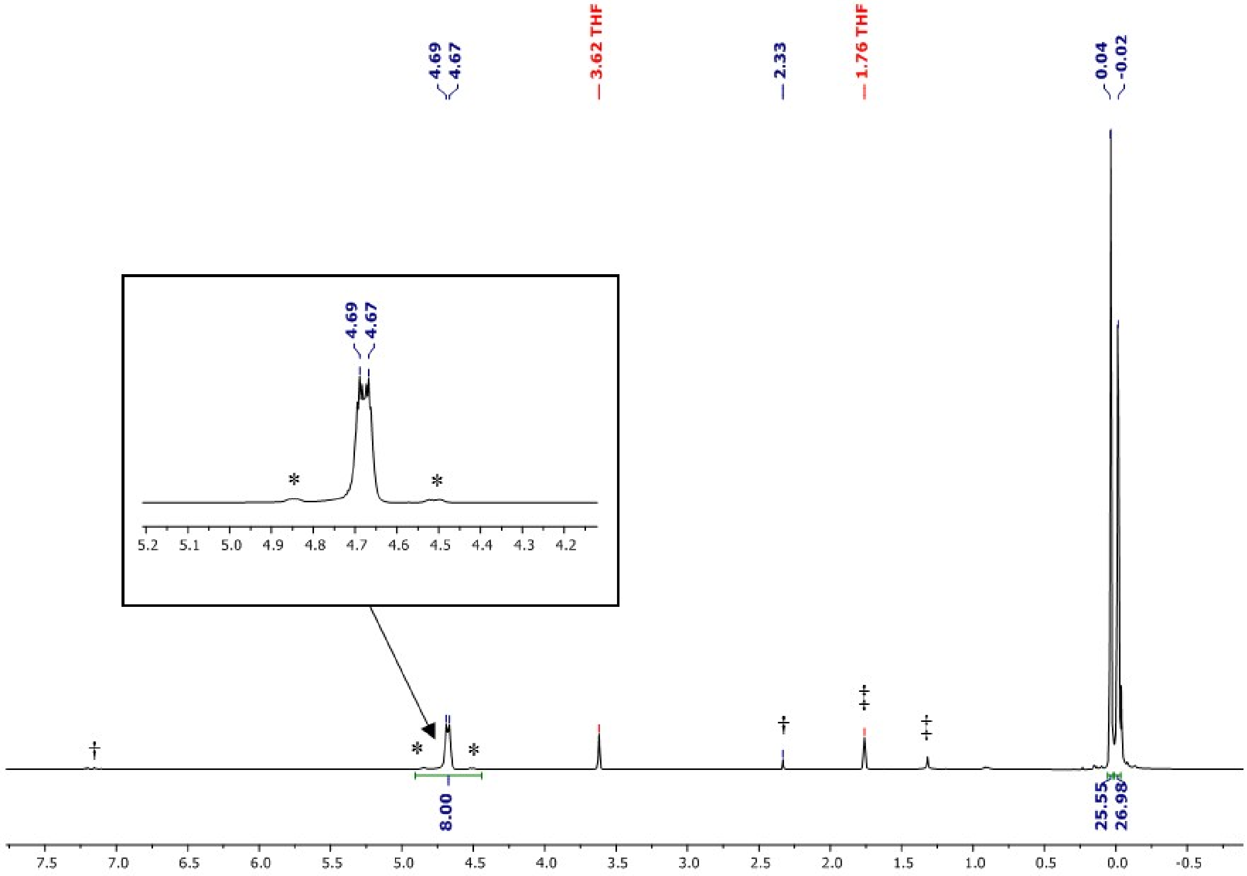

**Figure S1.** $^1$H NMR spectrum (thf-$d_8$, 298 K) of $[\mathrm{CaLi_2\{\mu^2\text{-}N(SiMe_2H)_2\}_4}]$ (**1**). † = residual toluene; ‡ = H grease; * = $^1J_{\mathrm{SiH}}$ satellites.

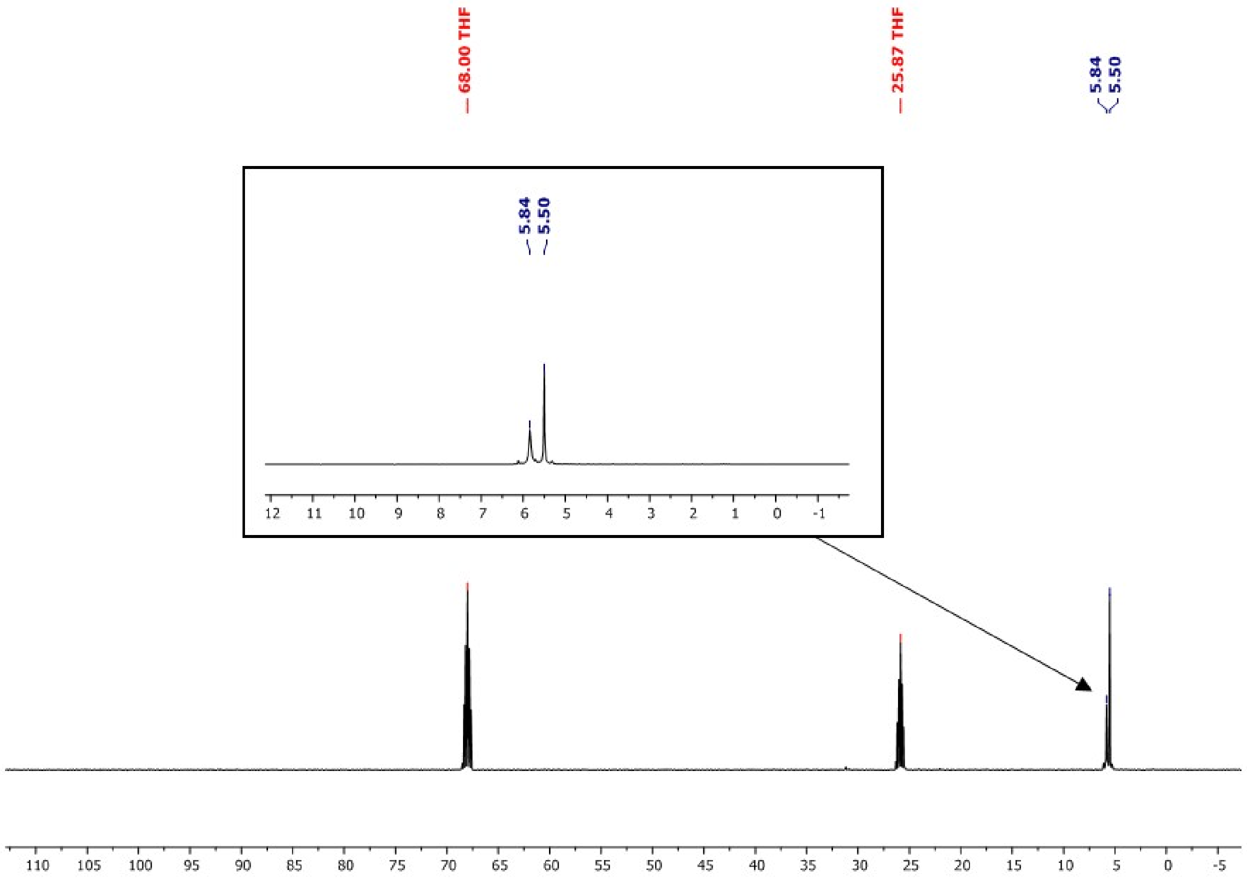

**Figure S2.** $^{13}C\{^{1}H\}$ NMR spectrum (thf-$d_8$, 298 K) of [CaLi$_2$\{μ$^2$-N(SiMe$_2$H)$_2$\}$_4$] (**1**).

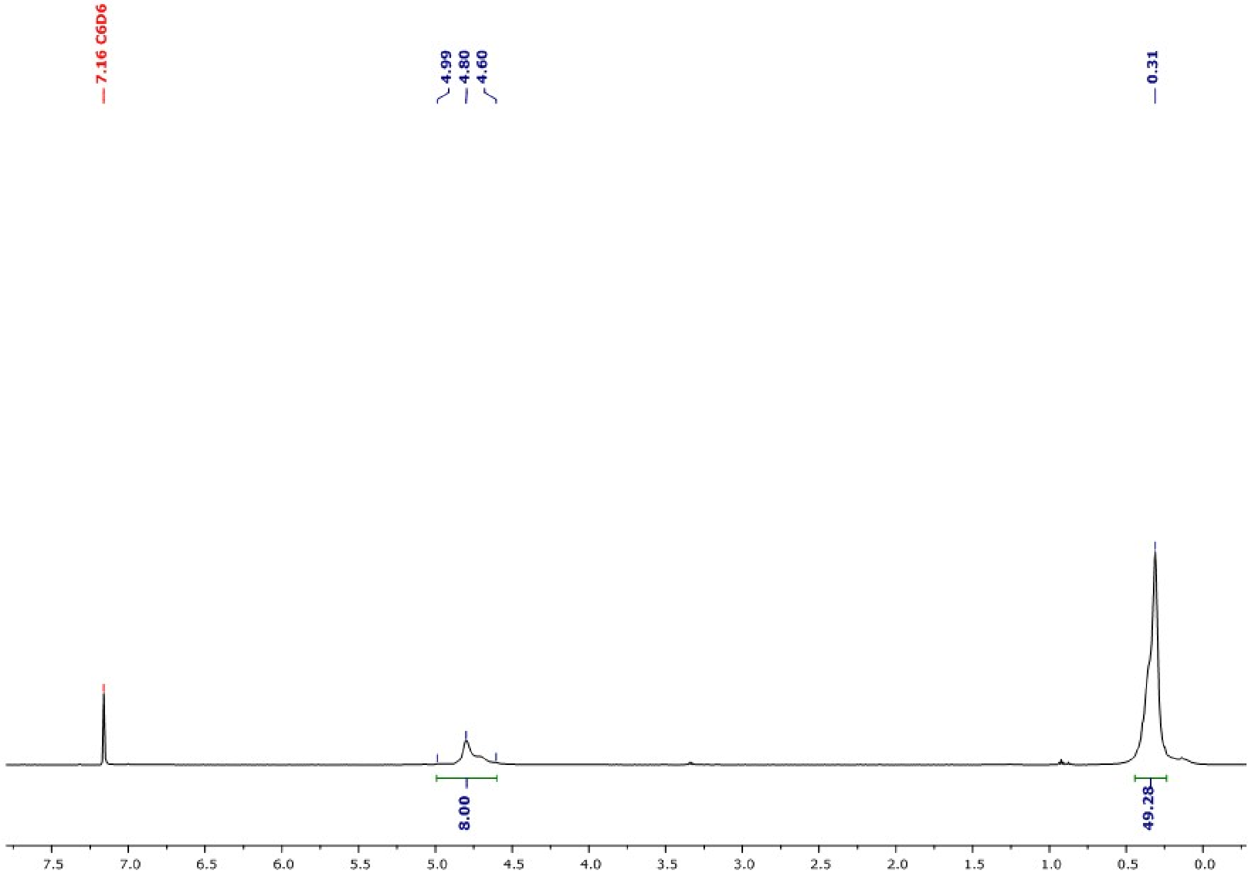

**Figure S3.** $^1$H NMR spectrum (benzene-*d*$_6$, 298 K) of [CaLi$_2${μ$^2$-N(SiMe$_2$H)$_2$}$_4$] (**1**).

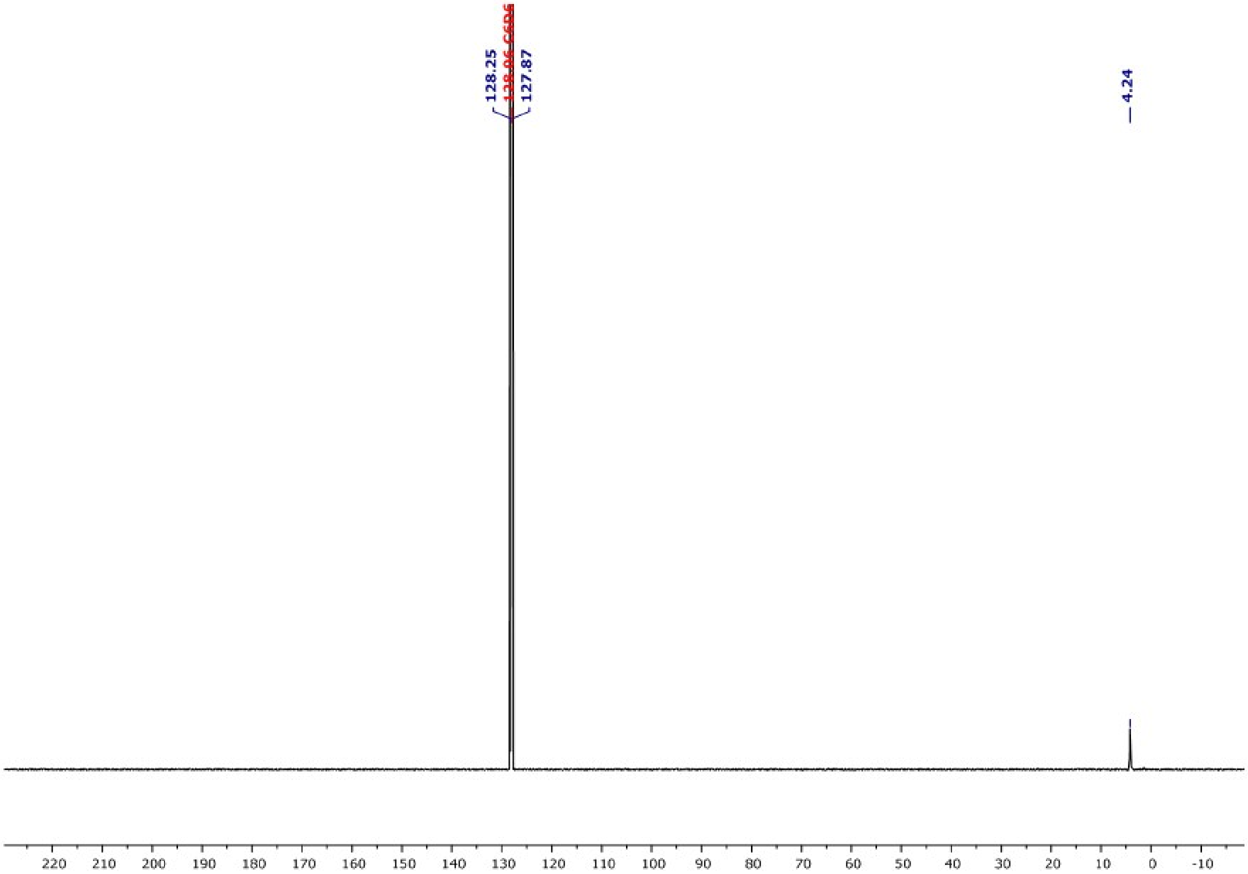

**Figure S4.** $^{13}C\{^1H\}$ NMR spectrum (benzene-$d_6$, 298 K) of [$CaLi_2\{\mu^2\text{-}N(SiMe_2H)_2\}_4$] (**1**).

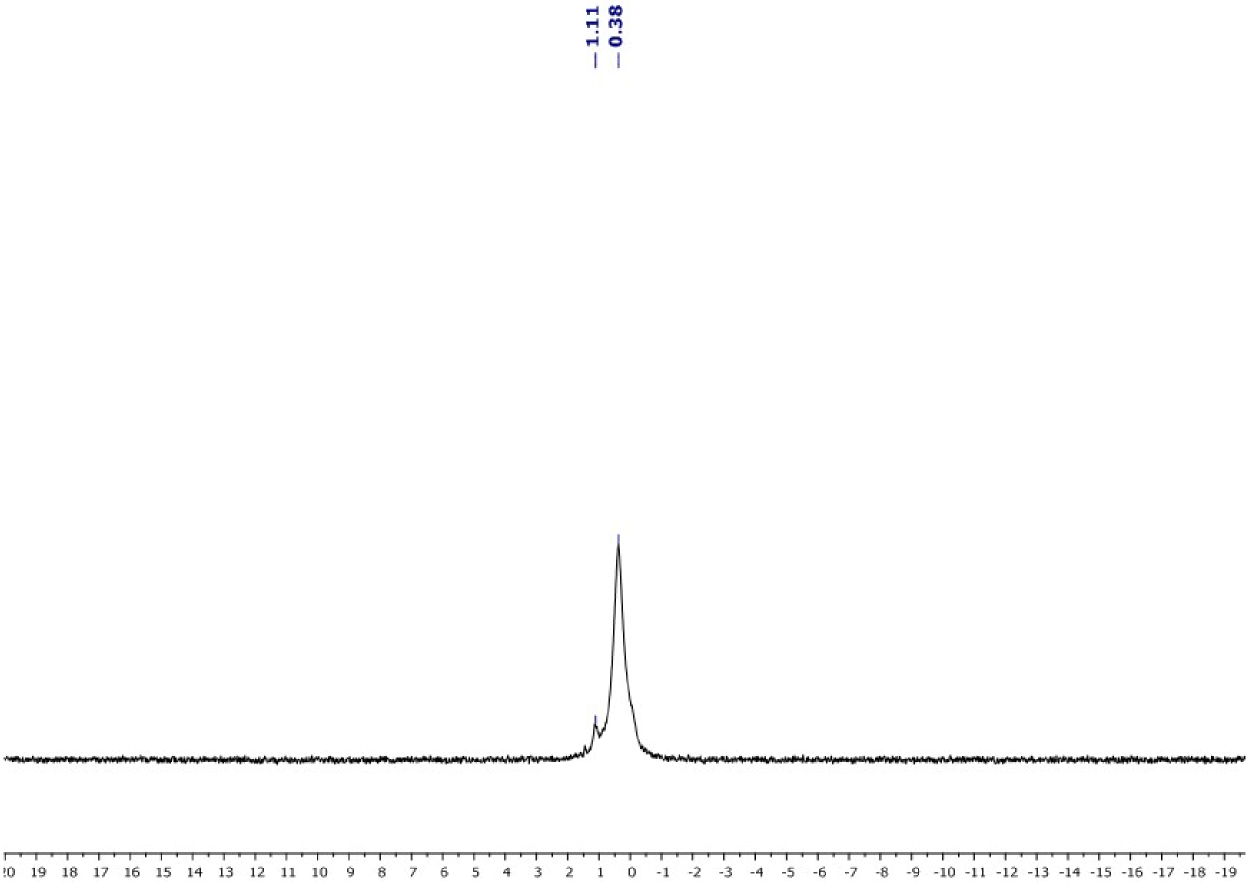

**Figure S5.** $^7$Li NMR spectrum (benzene-$d_6$, 298 K) of $[CaLi_2\{\mu^2\text{-}N(SiMe_2H)_2\}_4]$ (**1**).

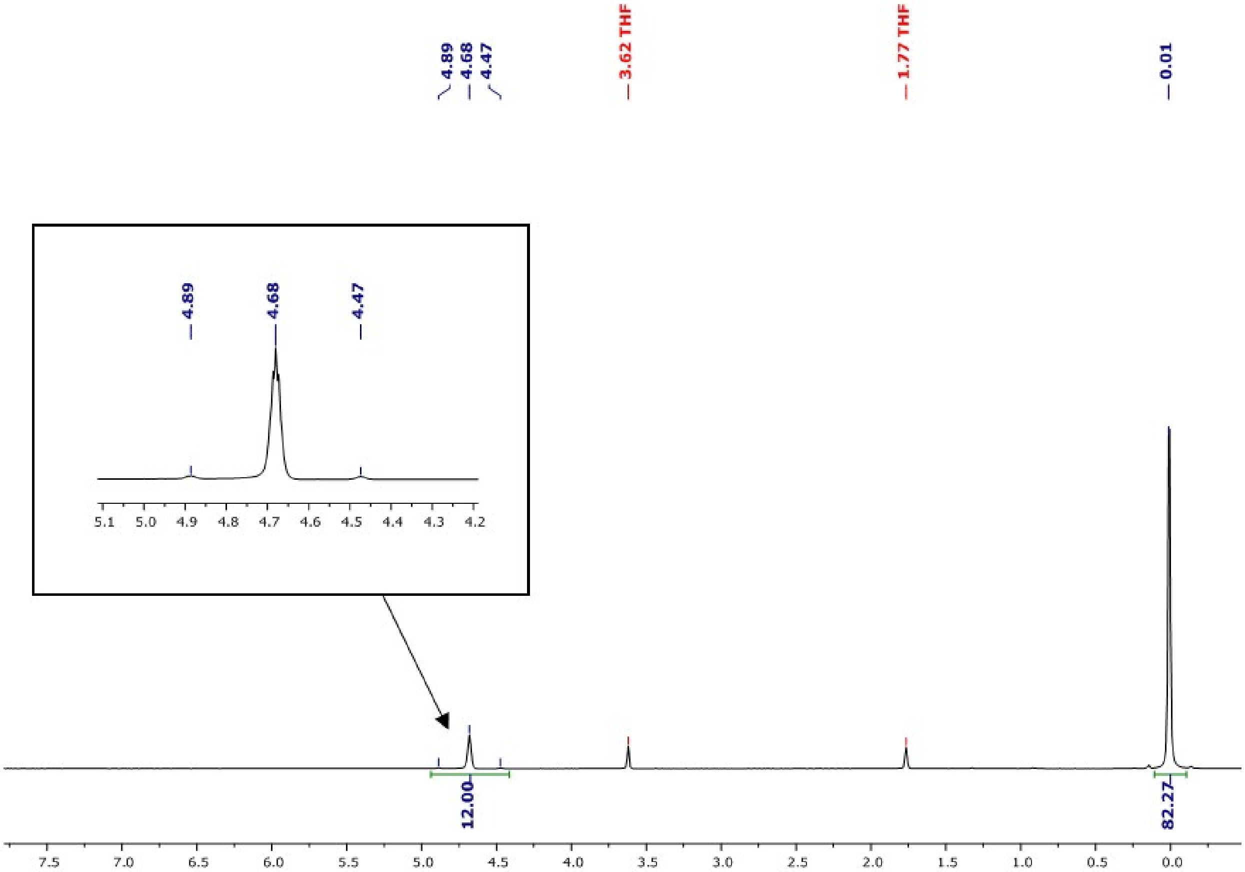

**Figure S6.** $^1$H NMR spectrum (thf-$d_8$, 298 K) of $[Ba_2Li_2\{\mu^2\text{-}N(SiMe_2H)_2\}_6]_\infty$ (**2**).

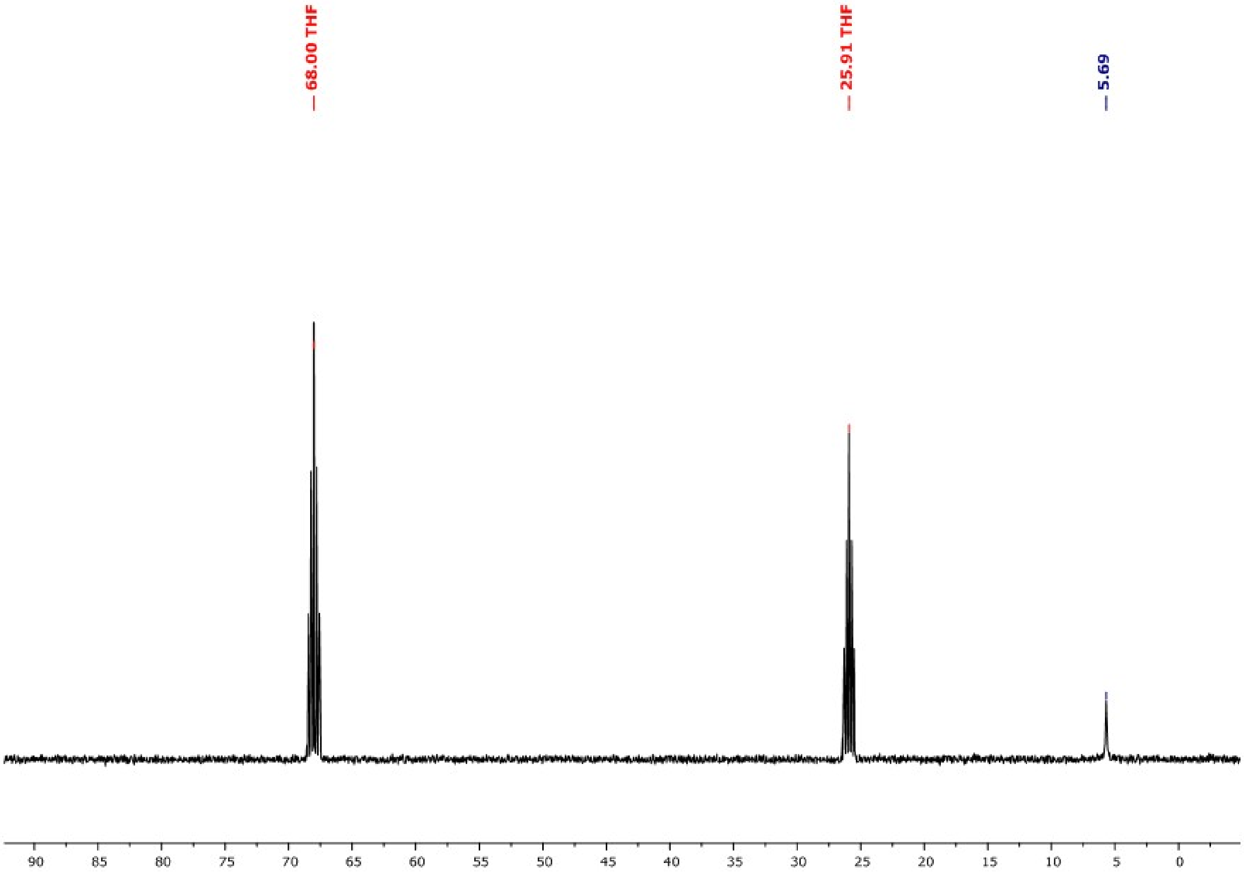

**Figure S7.** $^{13}C\{^1H\}$ NMR spectrum (thf-$d_8$, 298 K) of $[Ba_2Li_2\{\mu^2\text{-}N(SiMe_2H)_2\}_6]_\infty$ (**2**).

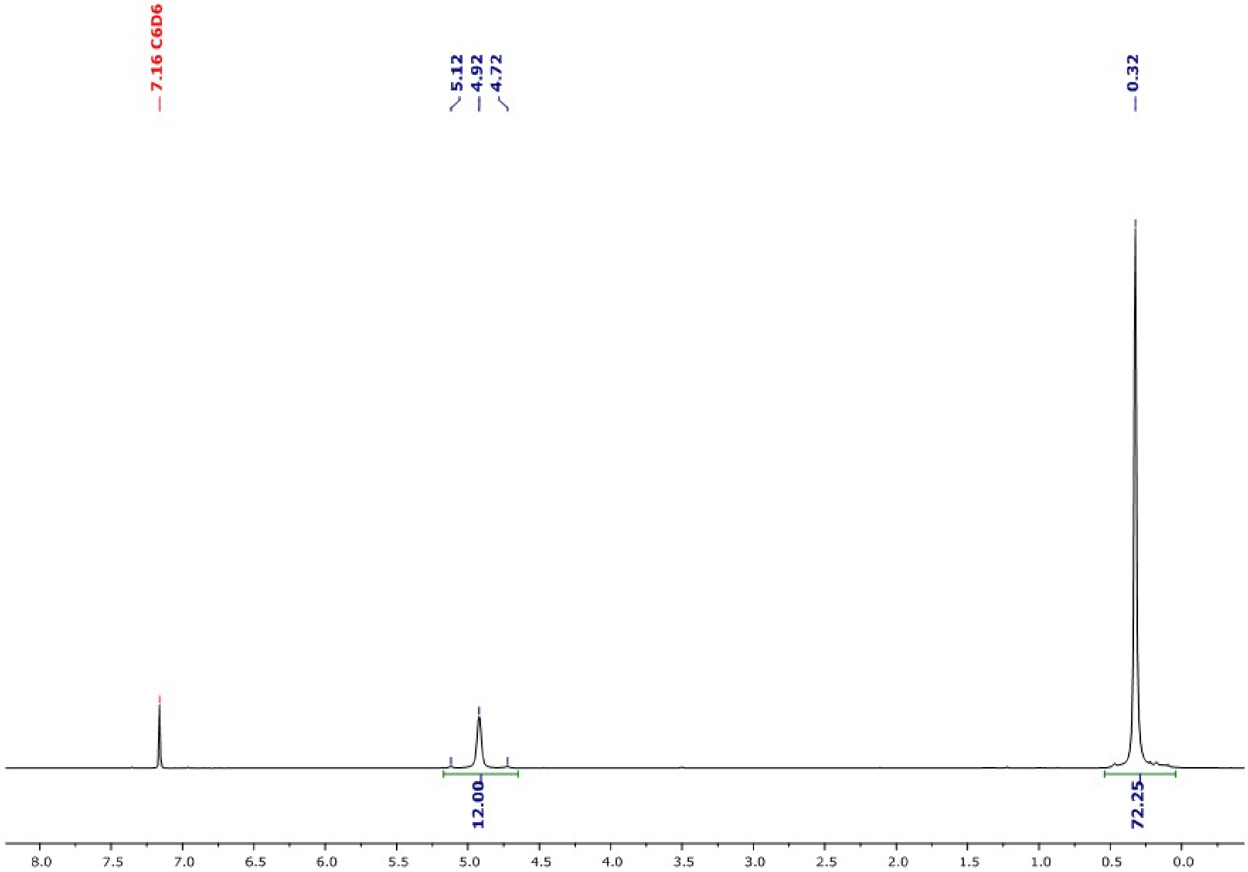

**Figure S8.** $^1$H NMR spectrum (benzene-$d_6$, 298 K) of $[Ba_2Li_2\{\mu^2\text{-}N(SiMe_2H)_2\}_6]_\infty$ (**2**).

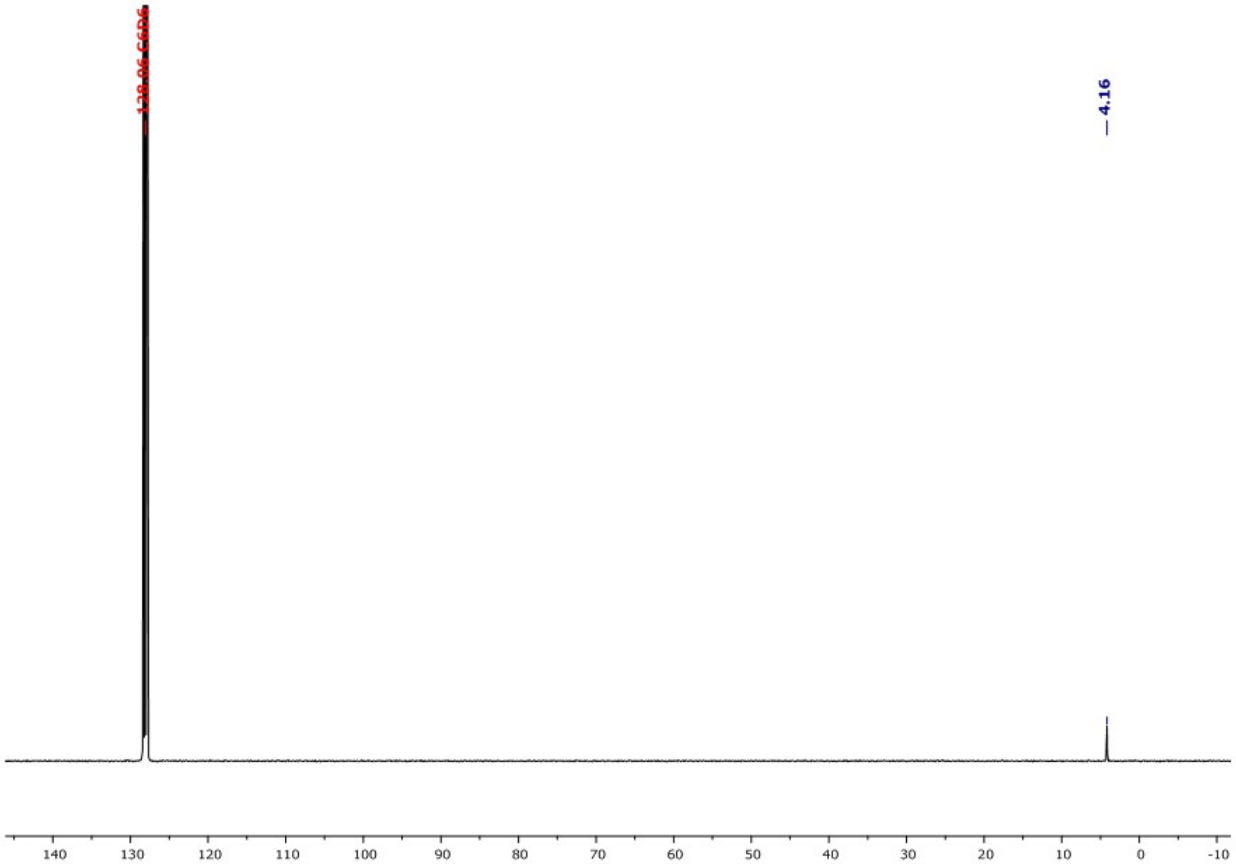

**Figure S9.** $^{13}C\{^1H\}$ NMR spectrum (benzene-$d_6$, 298 K) of $[Ba_2Li_2\{\mu^2\text{-}N(SiMe_2H)_2\}_6]_\infty$ (**2**).

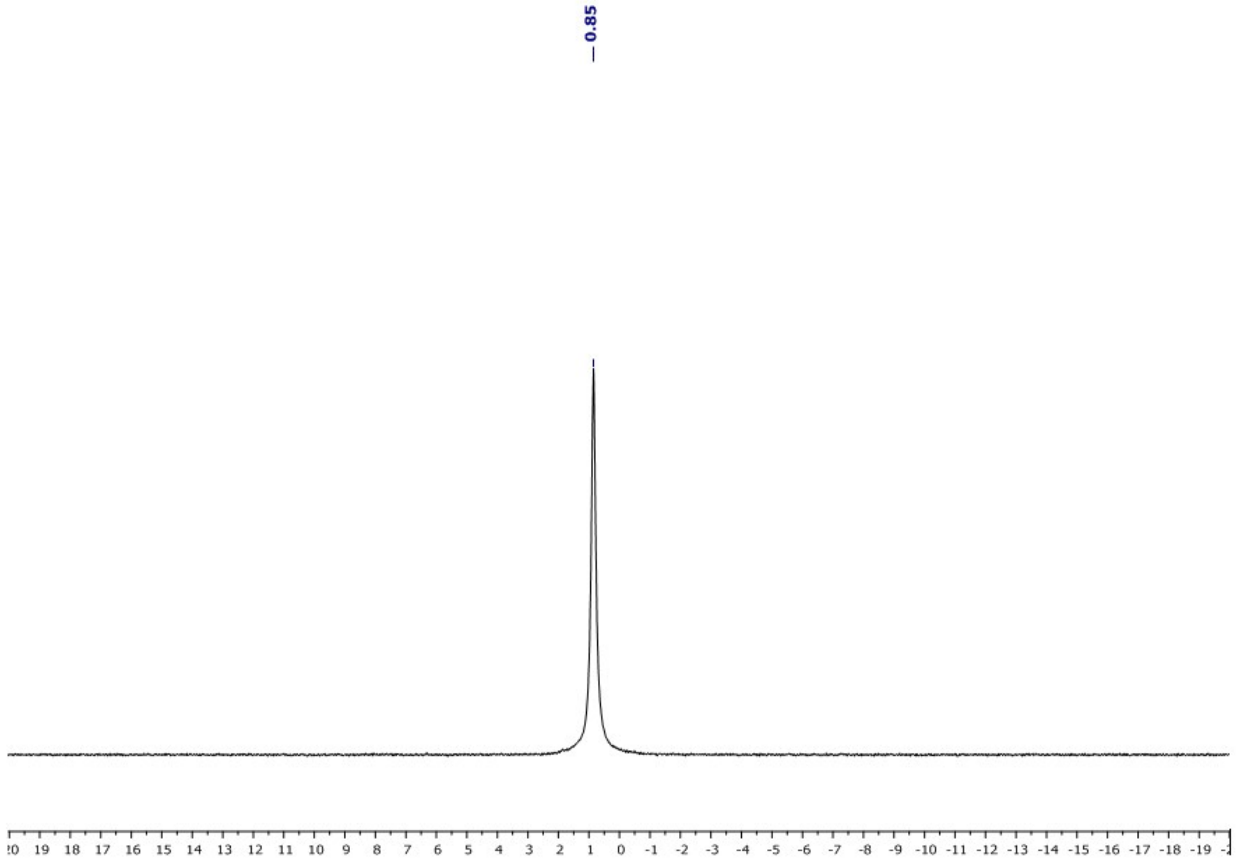

**Figure S10.** $^{7}$Li NMR spectrum (benzene-*d*$_6$, 298 K) of [Ba$_2$Li$_2${μ$^2$-N(SiMe$_2$H)$_2$}$_6$]$_\infty$ (**2**).

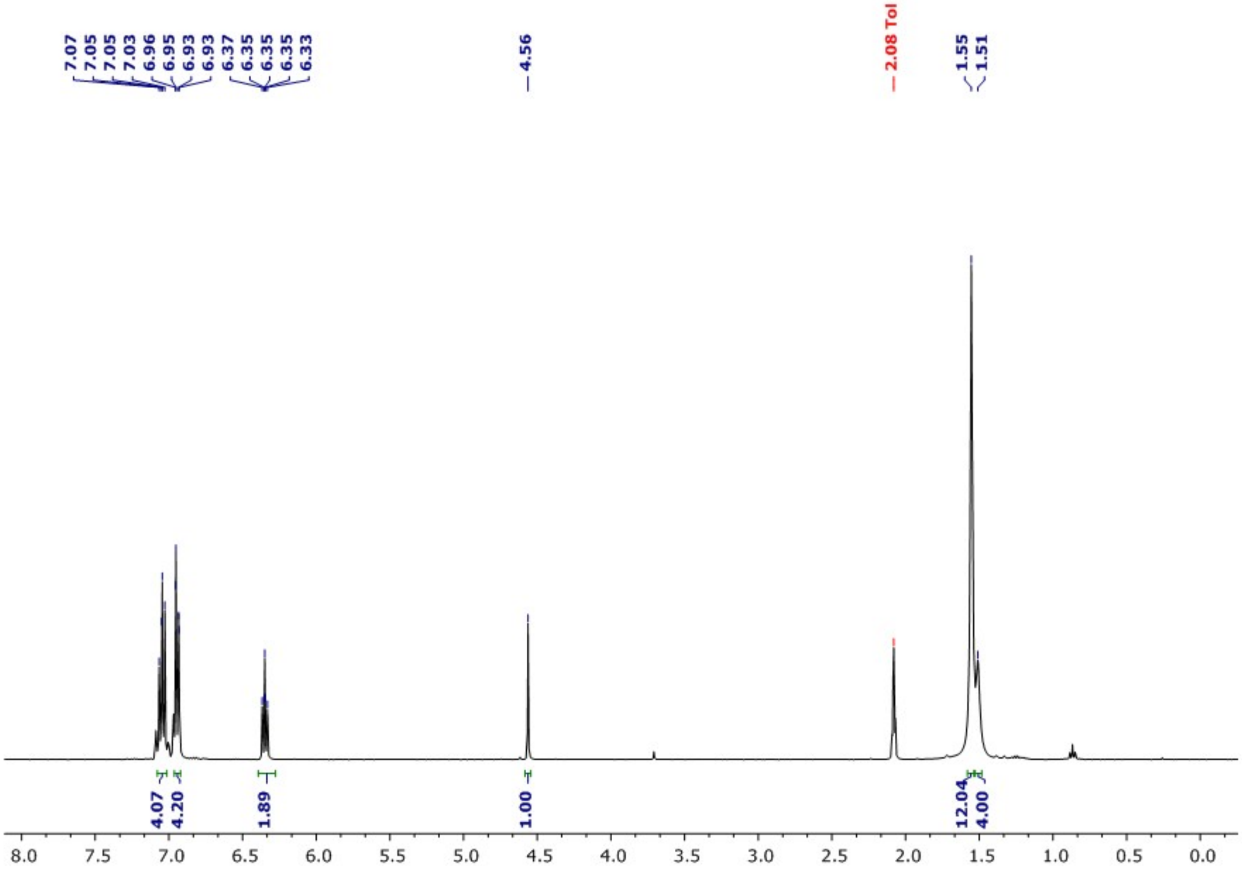

**Figure S11.** $^1$H NMR spectrum (toluene-$d_8$, 298 K) of [LiCHPh$_2$.tmeda].

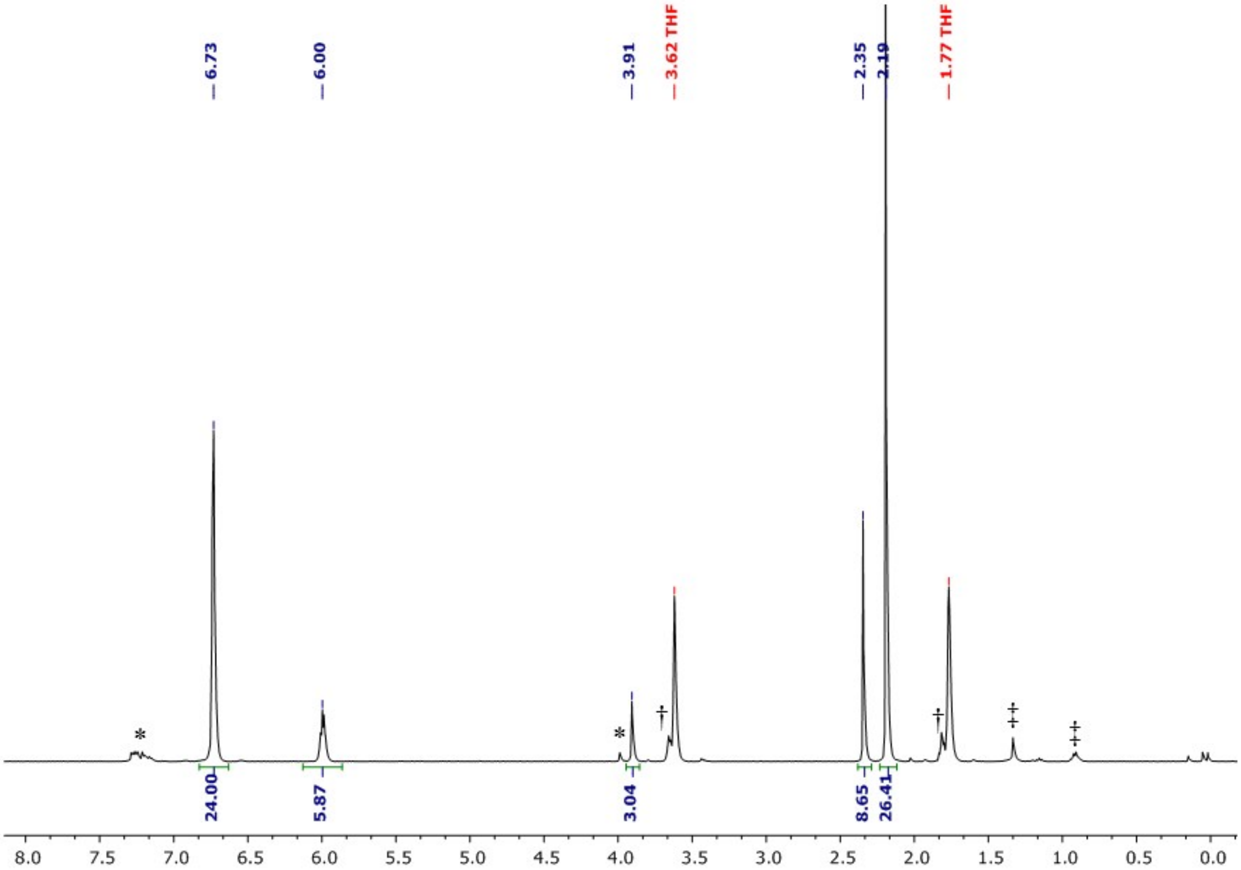

**Figure S12.** $^1$H NMR spectrum (298 K, thf-$d_8$) of [Li(tmeda)$_2^+$.Ca(CHPh$_2$)$_3$(thf)$^-$] (**3**). † = residual thf; ‡ = H grease; * = hydrolysed Ph$_2$CH$_2$.

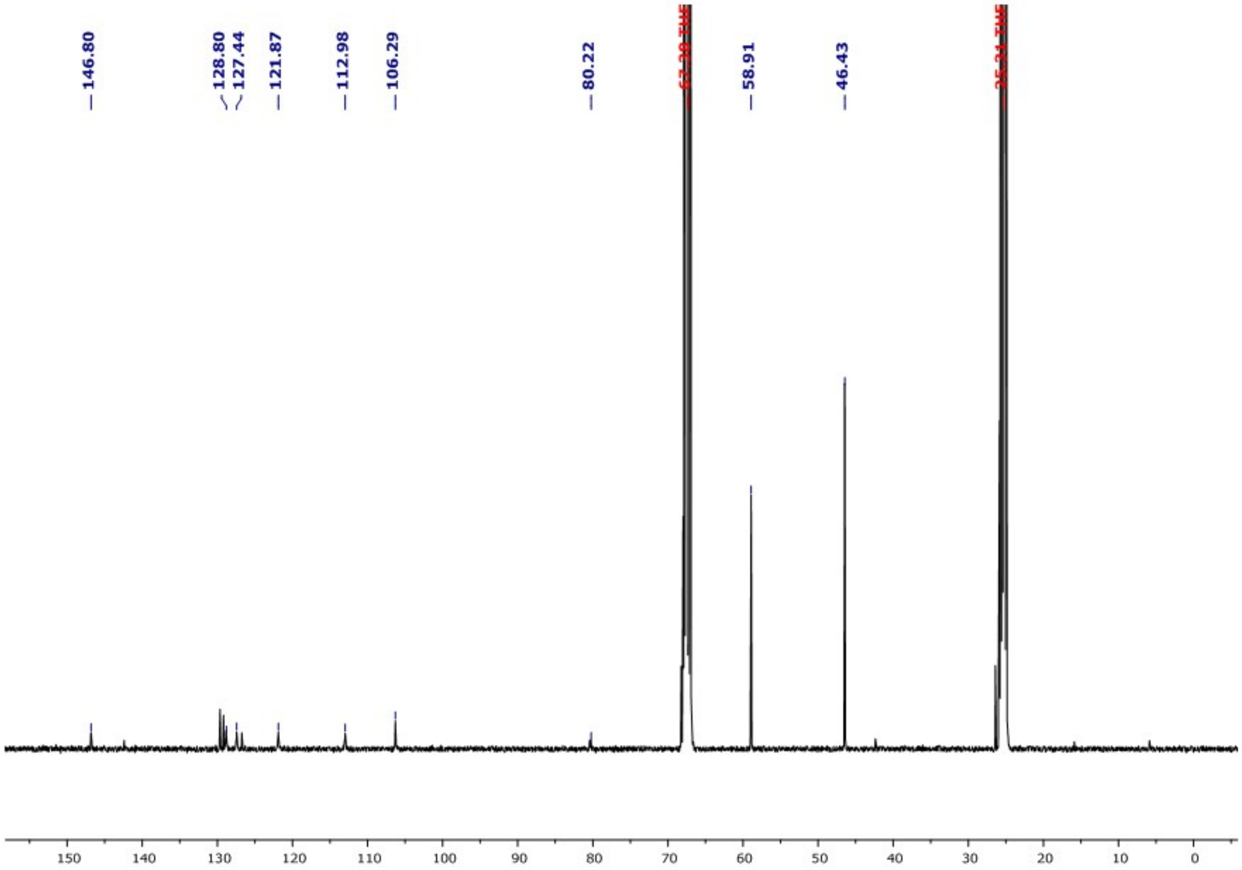

**Figure S13.** $^{13}C\{^1H\}$ NMR spectrum (213 K, thf-$d_8$) of [Li(tmeda)$_2^+$.Ca(CHPh$_2$)$_3$(thf)$^-$] (**3**).

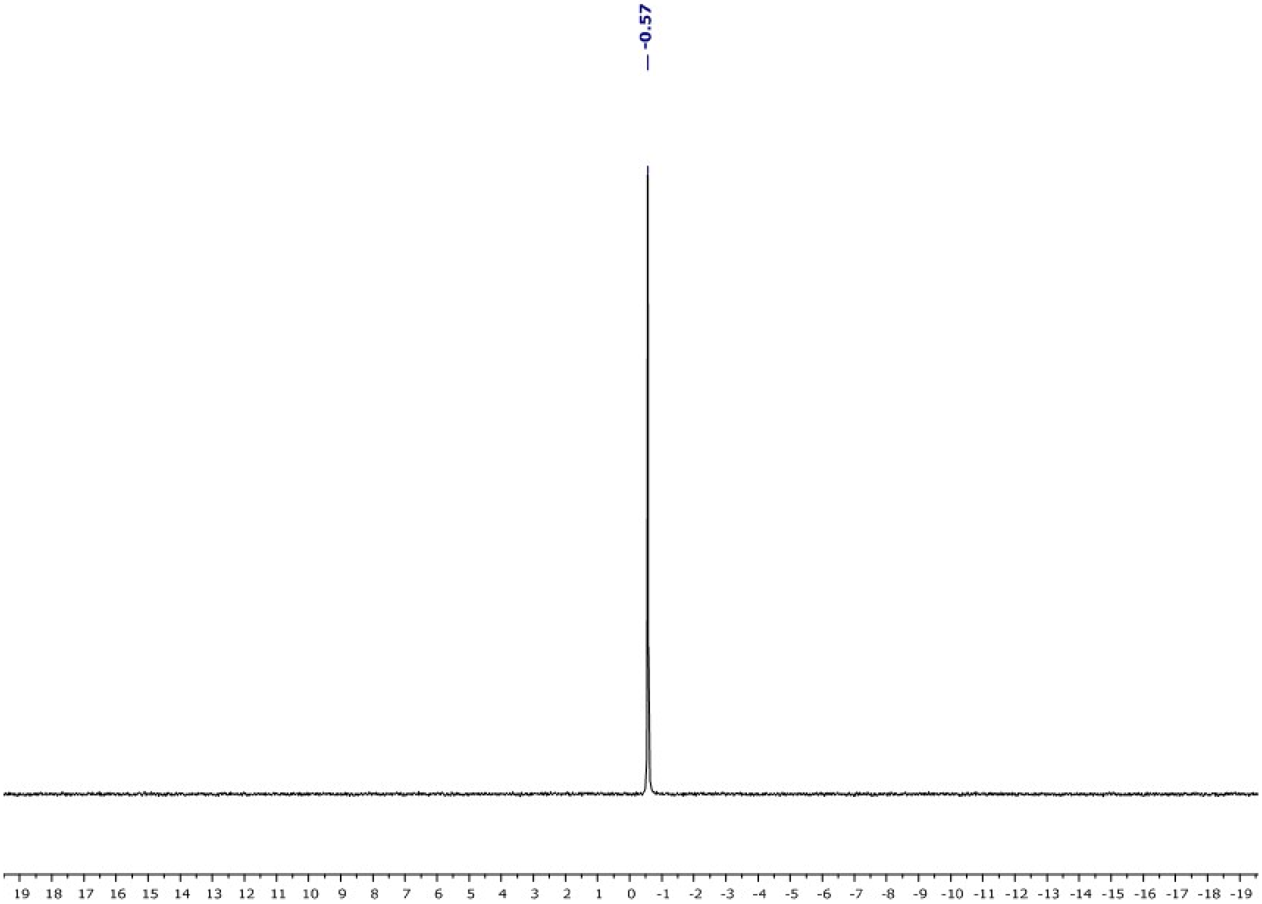

**Figure S14.** $^7$Li NMR spectrum (213 K, thf-$d_8$) of [Li(tmeda)$_2^+$.Ca(CHPh$_2$)$_3$(thf)$^-$] (**3**).

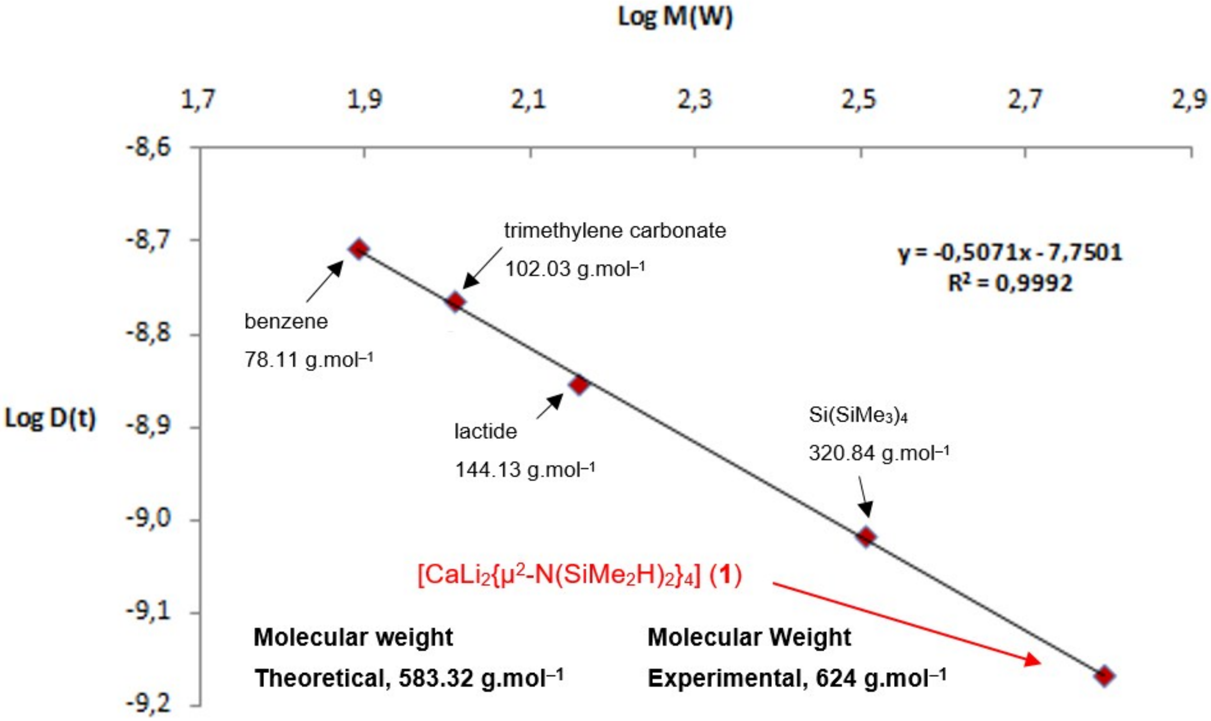

**Figure S15.** DOSY NMR (diffusion time - molecular weight analysis) for $[CaLi_2\{\mu^2\text{-}N(SiMe_2H)_2\}_4]$ (**1**). All NMR spectra recorded in benzene-$d_6$ at 298 K.

DOSY NMR measurements recorded at 25 °C with 0.08M solutions in benzene-$d_6$. Diffusion time vs. molecular weight analysis provides an estimated molecular weight of ca. 624 g.mol$^{-1}$ (theoretical mol. wt. 583.32 g.mol$^{-1}$, deviation ca. 7%).

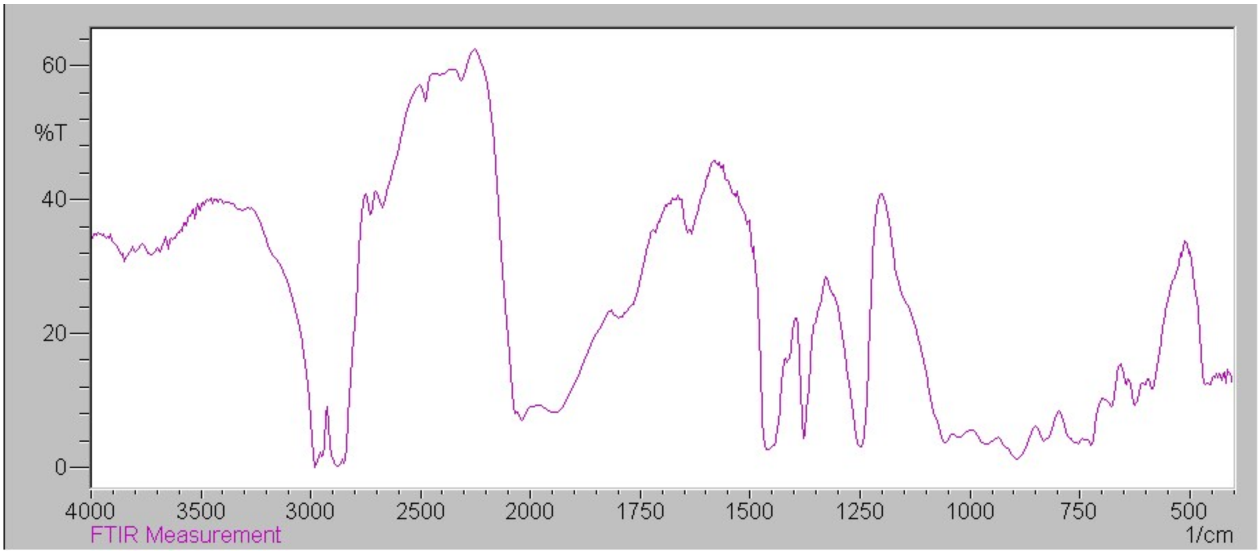

**Figure S16.** FTIR spectrum (Nujol mull in KBr plates) of $[\mathrm{CaLi_2\{\mu^2\text{-}N(SiMe_2H)_2\}_4}]_\infty$ (**1**).

Peak picking: 2034.90 (s), 1944.25 (s), 1797.66 (m), 1714.72 (w), 1631.78 (m), 1458.18 (s), 1415.75 (w), 1377.17 (s), 1247.94 (s), 1055.06 (s), 1026.13 (w), 962.48 (m), 893.04 (s), 833.28 (m), 752.24 (m), 677.01 (w), 624.94 (w), 584.43 (w) $\mathrm{cm^{-1}}$. Bands above 2300 $\mathrm{cm^{-1}}$ are only for Nujol.

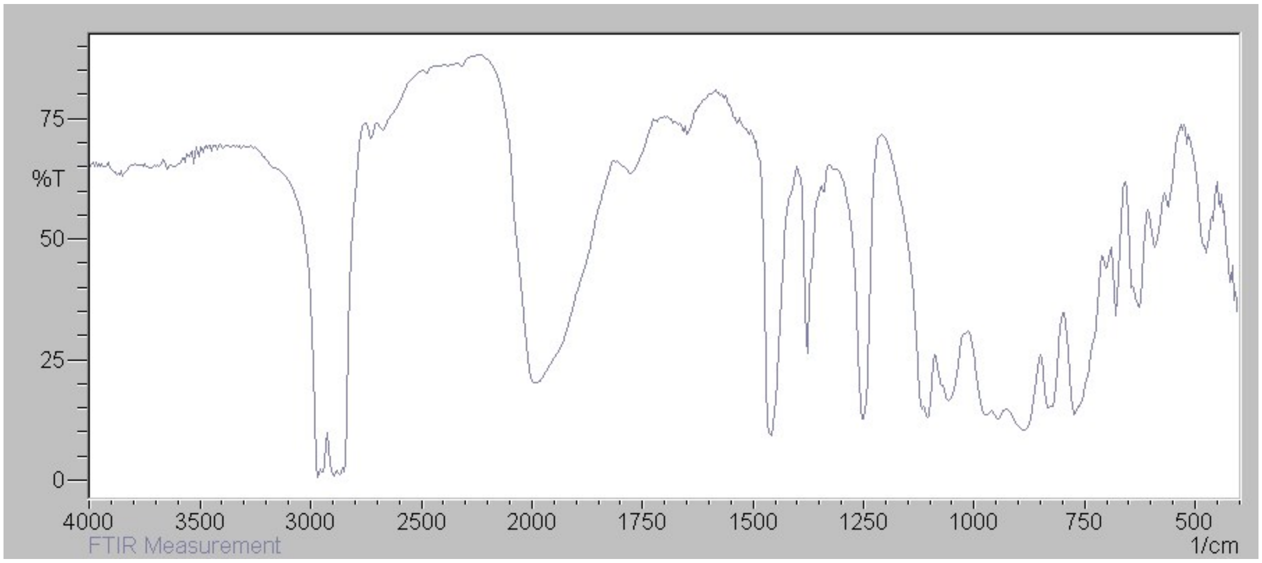

**Figure S17.** FTIR spectrum (Nujol mull in KBr plates) of $[Ba_2Li_2\{\mu^2\text{-}N(SiMe_2H)_2\}_6]_\infty$ (**2**).

Peak picking: 1994.40 (s), 1930.00 (sh), 1778.37 (m), 1649.14 (w), 1456.26 (s), 1411.88 (w), 1377.17 (s), 1340.53 (w), 1251.80 (s), 1103.28 (m), 1056.99 (m), 972.12 (s), 945.12 (s), 887.26 (m), 831.32 (m), 771.53 (s), 700.16 (w), 678.94 (m), 626.87 (m), 592.15 (m), 561.29 (w) cm$^{-1}$. Bands above 2300 cm$^{-1}$ are only for Nujol.

## X-ray diffraction crystallography

Crystals of complexes **1**-**3** (CCDC 1896015-1896017) suitable for X-ray diffraction analysis were obtained by crystallisation in toluene (**1** and **2**) or in the bulk (**3**). Diffraction data were collected at 150 K using a D8 VENTURE Bruker AXS diffractometer with graphite-monochromated MoKα radiation ($\lambda = 0.71073$ Å). Relevant collection and refinement data are summarised in Table S1.

The structure of **1** was solved by dual-space algorithm using the *SHELXT* program, and then refined with full-matrix least-square methods based on $F^2$ (*SHELXL-2014*). All non-hydrogen atoms were refined with anisotropic atomic displacement parameters. Except silicon linked hydrogen atoms that were introduced in the structural model through Fourier difference maps analysis, H atoms were finally included in their calculated positions. A final refinement on $F^2$ with 4084 unique intensities and 161 parameters converged at $\omega R(F^2) = 0.0792$ ($R(F) = 0.0334$) for 3574 observed reflections with $I > 2\sigma(I)$.

The structure of **2** was solved by dual-space algorithm using the *SHELXT* program, and then refined with full-matrix least-squares methods based on $F^2$ (*SHELXL*). All non-hydrogen atoms were refined with anisotropic atomic displacement parameters. Except Si linked hydrogen atoms that were introduced in the structural model through Fourier difference maps analysis, H atoms were finally included in their calculated positions and treated as riding on their parent atom with constrained thermal parameters. A final refinement on $F^2$ with 12579 unique intensities and 463 parameters converged at $\omega R(F^2) = 0.0908$ ($R(F) = 0.0374$) for 11362 observed reflections with $I > 2\sigma(I)$.

The structure of **3** was solved by dual-space algorithm using the SHELXT program,[2] and then refined with full-matrix least-square methods based on F2 (SHELXL-2014).[3] All non-hydrogen atoms were refined with anisotropic atomic displacement parameters. H atoms were finally included in their calculated positions. A final refinement on $F^2$ with 12758 unique intensities and 625 parameters converged at $\omega R(F^2) = 0.1583$ ($R(F) = 0.0597$) for 10218 observed reflections with $I > 2\sigma(I)$.

**Table S18.** Crystal data and structure refinement for **1-3**

| | **$[CaLi_2\{\mu^2\text{-}N(SiMe_2H)_2\}_4]_\infty$ (1)** | **$[Ba_2Li_2\{\mu^2\text{-}N(SiMe_2H)_2\}_6]_\infty$ (2)** | **$[Li(tmeda)_2^+.Ca(CHPh_2)_3(thf)^-]$ (3)** |
|---|---|---|---|
| CCDC number | 1896015 | 1896016 | 1896017 |
| Formula | $C_{16}H_{56}CaLi_2N_4Si_8$ | $C_{24}H_{84}Ba_2Li_2N_6Si_{12}$ | $C_{59}H_{83}CaLiN_4O_2$ |
| Mol. wt | 583.32 | 1082.61 | 927.31 |
| Crystal system | Orthorhombic | Monoclinic | Monoclinic |
| Space group | P b c n | P $2_1$/n | P $2_1$/n |
| a [Å] | 17.8573 (8) | 16.8123(18) | 13.991(2) |
| b [Å] | 11.1476(5) | 11.6250(13) | 25.818(3) |
| c [Å] | 17.9233(7) | 28.427(3) | 15.859(2) |
| α [°] | 90 | 90 | 90 |
| β [°] | 90 | 96.337(4) | 103.450(5) |
| γ [°] | 90 | 90 | 90 |
| V [Å$^3$] | 3567.9(3) | 5521.9(11) | 5571.6(13) |
| Z | 4 | 4 | 4 |
| Density (g cm$^{-3}$) | 1.086 | 1.302 | 1.105 |
| Abs. coeff., (mm$^{-1}$) | 0.457 | 1.700 | 0.156 |
| F(000) | 1272 | 2224 | 2016 |
| Crystal size, mm | 0.400 × 0.320 × 0.200 | 0.300 × 0.150 × 0.100 | 0.350 × 0.300 × 0.200 |
| θ range [°] | 3.132 to 27.479 | 2.942 to 27.484 | 2.944 to 27.483 |
| Limiting indices | $23 < h < 22$ | $18 < h < 21$ | $18 < h < 18$ |
| | $10 < k < 14$ | $15 < k < 15$ | $28 < k < 33$ |
| | $23 < l < 23$ | $36 < l < 36$ | $20 < l < 20$ |
| R(int) | 0.0285 | 0.0322 | 0.0439 |
| Reflections collected | 16794 / 4084 | 62936 / 12579 | 83760 / 12758 |
| Refl. Unique [$I > 2\sigma(I)$] | 3574 | 11362 | 10218 |
| Completeness to θ | 0.998 | 0.993 | 0.999 |
| Data/ restraints/ param. | 4084 / 0 / 161 | 12579 / 2 / 463 | 12758 / 0 / 625 |
| Goodness-of-fit | 1.109 | 1.146 | 1.021 |
| $R_1$ [$I > 2\sigma(I)$] (all data) | 0.0334 (0.0407) | 0.0374 (0.0429) | 0.0597 (0.0754) |
| $wR_2$ [$I > 2\sigma(I)$] (all data) | 0.0792 (0.0849) | 0.0908 (0.0936) | 0.1583 (0.1728) |
| Largest diff. [e A$^{-3}$] | 0.742 and -0.413 | 1.193 and -1.064 | 0.902 and -0.489 |

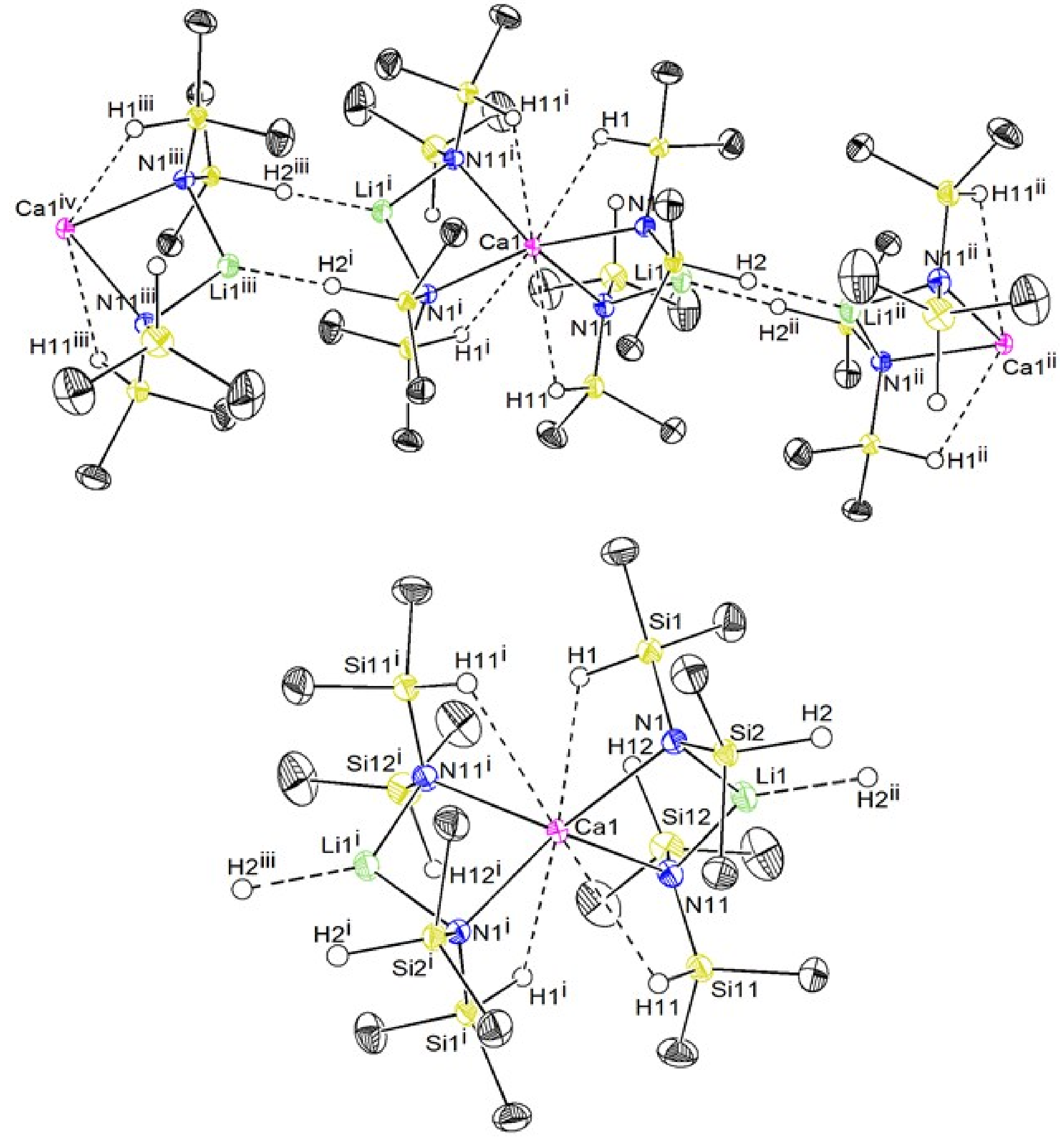

**Figure S19.** ORTEP representation of the solid-state structure of $[\mathrm{CaLi_2\{\mu^2\text{-}N(SiMe_2H)_2\}_4}]_\infty$ (**1**), showing the repetitive motif along the 1-D coordination polymer (top) and the details of the coordination sphere around the $\mathrm{CaLi_2}$ core (bottom). Ellipsoids drawn at the 50% probability level. H atoms other than Si*H* omitted for clarity. Ca···H and Li···H depicted in dotted lines. Colour code: Ca, magenta; Li, green; Si, gold; N, blue; C, black.

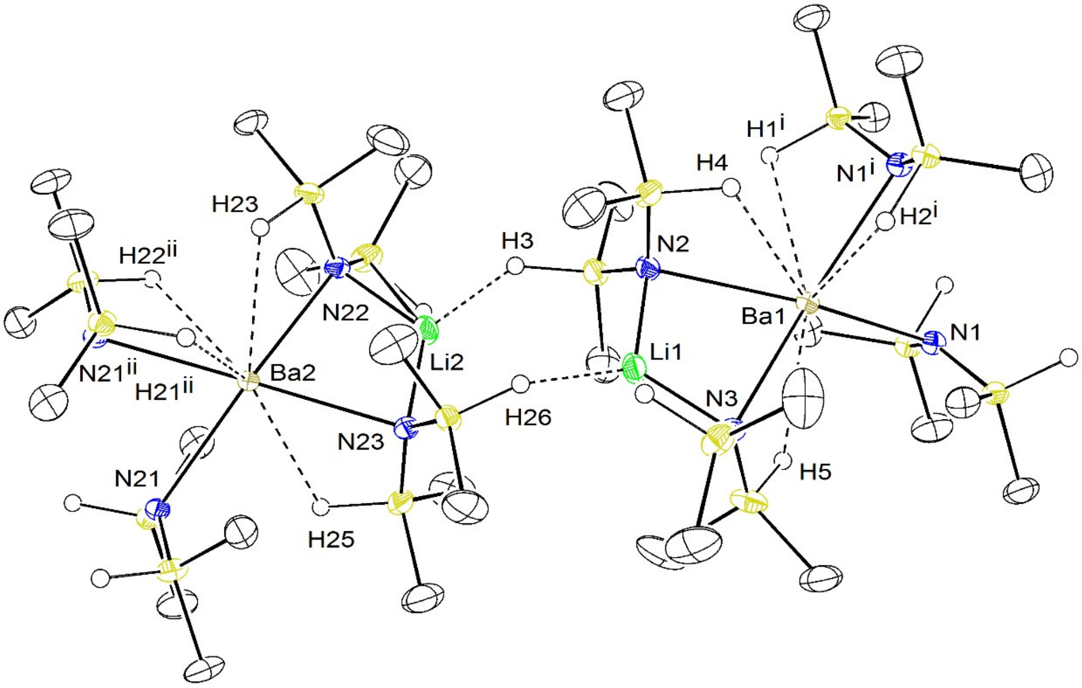

**Figure S20.** ORTEP representation of the solid-state structure of $[Ba_2Li_2\{\mu^2\text{-}N(SiMe_2H)_2\}_6]_\infty$ (**2**). Ellipsoids drawn at the 50% probability level. H atoms other than Si*H* omitted for clarity. Ba···H and Li···H depicted in dotted lines. Colour code: Ba, brown; Li, green; Si, gold; N, blue; C, black.

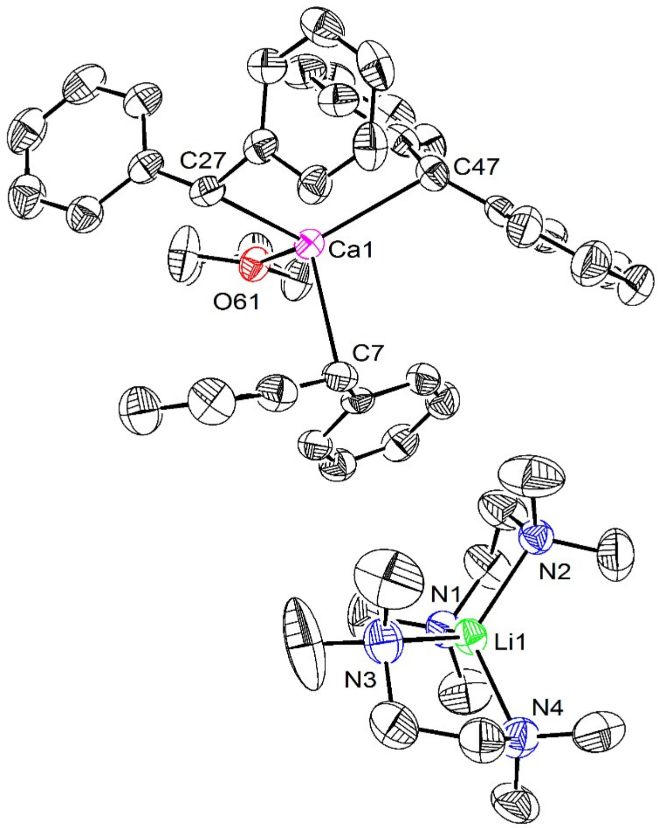

**Figure S21.** ORTEP representation of the solid-state structure of [Li(tmeda)$_2^+$.Ca(CHPh$_2$)$_3$(thf)$^-$] (**3**). Ellipsoids drawn at the 50% probability level. Non-interacting Et$_2$O molecule and H atoms omitted for clarity. Only the main component of disordered thf and tmeda molecules are drawn. Colour code: Ca, magenta; Li, green; N, blue; C, black; O, red.

## References

1 (*a*) Y. Sarazin, D. Roşca, V. Poirier, T. Roisnel, A. Silvestru, L. Maron and J.-F. Carpentier, *Organometallics*, 2010, **29**, 6569; (*b*) N. Romero, S.-C. Roşca, Y. Sarazin, J.-F. Carpentier, L. Vendier, S. Mallet-Ladeira, C. Dinoi and M. Etienne, *Chem. Eur. J.*, 2015, **21**, 4115.

2 G. M. Sheldrick, *Acta Cryst. A*, 2015, **71**, 3.

3 G. M. Sheldrick, *Acta Cryst. C*, 2015, **71**, 3.